

ISSN 0042-6822
Volume 268, Number 1, March 1, 2000

VIROLOGY



ACADEMIC
PRESS

A Harcourt Science and
Technology Company



Loss of ATM Function Enhances Recombinant Adeno-Associated Virus Transduction and Integration through Pathways Similar to UV Irradiation

Salih Sanlioglu,* Peter Benson,† and John F. Engelhardt*^{†1}

*Departments of Anatomy and Cell Biology and of Internal Medicine, †Center for Gene Therapy, and ‡Department of Otolaryngology, University of Iowa School of Medicine, Iowa City, Iowa 52242

Received August 13, 1999; returned to author for revision October 5, 1999; accepted December 13, 1999

Ataxia telangiectasia is caused by a genetic defect in the ATM gene that results in altered cellular sensitivity to DNA-damaging agents such as γ -irradiation. ATM deficiency is associated with an increased incidence of neurological disorders, immune deficiency, and cancer. In this report we demonstrate that recombinant adeno-associated virus (rAAV) gene transfer in ATM-deficient fibroblasts is significantly enhanced over normal fibroblast cell lines. This enhancement of rAAV transduction in AT cells is correlated with an increased abundance of circular form rAAV genomes, as well as a higher number of integrated head-to-tail concatamer proviral genomes. Studies evaluating AAV trafficking using Cy3-labeled virus suggest that a nuclear mechanism is responsible for increased rAAV transduction in AT cells, because binding, endocytosis, and nuclear trafficking of virus are unaffected by the AT phenotype. Additionally, the profile of rAAV transduction after UV irradiation is significantly blunted in AT cells, suggesting that the level of DNA repair enzymes normally associated with UV augmentation of viral transduction may already be maximally elevated. These results further expand our understanding of genes involved in rAAV transduction. © 2000 Academic Press

INTRODUCTION

DNA damage manifested as double-stranded breaks occurs frequently on exposure to chemical carcinogens and radiation. For the maintenance of genomic integrity, these errors must be recognized and repaired effectively. When these processes are impaired, inaccurate restoration of the genome leads to mutations that may result in cell death or cancer. Ataxia telangiectasia is a human autosomal recessive disease characterized by neurological disorders (cerebellar ataxia), immune deficiency, and a predisposition to cancer (Shiloh, 1995, 1997). Importantly, chromosomal instability has been recognized as the most detrimental characteristic of the AT phenotype (Luo et al., 1996).

The ATM gene, which was recently isolated by positional cloning (Savitsky et al., 1995), has strong homology to proteins of the phosphatidylinositol 3-kinase (PI-3) family (Jung et al., 1997). PI-3 kinases mediate cellular responses to several mitogenic growth factors (Kapeller and Cantley, 1994; Ui et al., 1995; Whitman et al., 1988). Interestingly, ATM is a protein kinase rather than a lipid kinase (Banin et al., 1998; Canman et al., 1998), and it has been shown to regulate the p53-dependent cell cycle checkpoint and apoptotic pathways (Barlow et al., 1997; Nakamura, 1998). In wild-type cells, ATM activates p53 through phosphorylation (Banin et al., 1998), and consequently the cell cycle is arrested and DNA repair path-

ways are activated (Kastan et al., 1992; Lu et al., 1998). p53 can also be activated by ionizing and UV irradiation. Interestingly, sensitivity to UV and ionizing radiation appears to be altered in AT patients, because the onset of p53 activation is delayed after ionizing but not UV irradiation. Although both UV and ionizing radiation result in the phosphorylation of p53 protein, ionizing radiation results in phosphorylation at serine-15 and UV radiation at serine-389. These differences may account for the differential effects of these two stimuli on AT cells (Canman et al., 1998; Lu et al., 1998).

Adeno-associated virus 2 (AAV2) is one of the most promising gene therapy vectors currently available. It is a human parvovirus with a single-stranded DNA (ssDNA) genome (Berns, 1990). Transduction of nondividing cells, site-specific integration, and nonpathogenic features have made rAAV the vector of choice for many applications in gene therapy (Flotte et al., 1994; Kaplitt et al., 1994; Kotin et al., 1991; McCown et al., 1996; Walsh et al., 1992). Despite these advantages, the low level of viral transduction in certain organs has been one of the biggest barriers in rAAV gene therapy trials. Therefore, methods of augmenting rAAV transduction would greatly increase its applications as a gene therapy vector. In addition to DNA synthesis and topoisomerase inhibitors, DNA damaging agents such as UV and γ -irradiation have been suggested to augment rAAV transduction (Alexander et al., 1994; Russell et al., 1995). The mechanism of action for these agents is not clearly understood but is thought to involve the activation of DNA repair machinery following DNA damage (Alexander et al., 1994).

¹ To whom reprint requests should be addressed at 51 Newton Road, Room 1-111 BSB. Fax: (319) 335-7198.

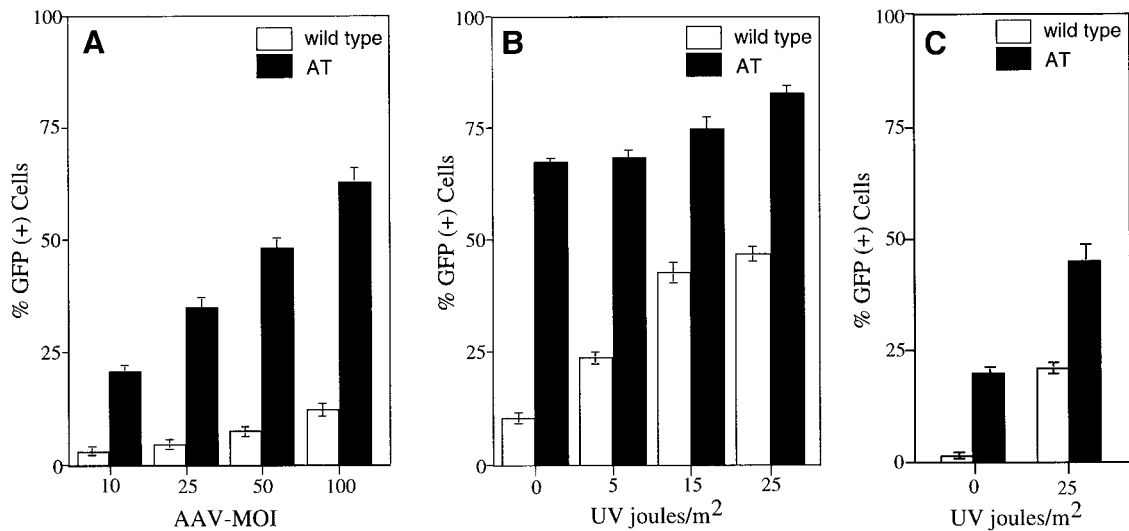


FIG. 1. rAAV transduction in AT and wild-type fibroblasts. Confluent monolayers of wild-type (GM637) and AT (GM5849)-transformed fibroblasts were infected with increasing m.o.i. values of AV.GFP3ori (A). The percentage of cells expressing GFP was determined by FACS analysis 24 h after the infections. These data represent the mean \pm SEM of six independent data points ($n = 6$). (B) Results from UV-induced rAAV transduction in wild-type (GM637) and in AT (GM5849) fibroblast cell lines. AT (GM5849) and wild-type (GM637) fibroblasts were UV irradiated at increasing doses (0, 5, 15, and 25 J/m²) before infection with AV.GFP3ori at an m.o.i. of 100 DNA particles/cell. The percentage of cells expressing GFP was determined 24 h after the UV irradiation by FACS analysis. These data represent the mean \pm SEM of four independent data points ($n = 4$). (C) rAAV transduction data in three independent primary AT (GM01740A, GM01829A, GM00648C) and wild-type (GM00023, GM00041B, GM00495A) fibroblast lines. Fibroblasts were infected with AV.GFP3ori at an m.o.i. of 200 DNA particles/cell with and without prior UV irradiation at 25 J/m². Assays were performed in triplicate, and transduction was analyzed at 4 days postinfection by FACS analysis. Results depict the mean \pm SEM for all three cell lines ($n = 9$ data points for each).

Given the correlation between ionizing radiation-induced rAAV transduction and the sensitivity of AT cells to ionizing radiation (Taylor *et al.*, 1975), we hypothesized that cell lines displaying radiation sensitivity or defective DNA repair pathways might have altered profiles of rAAV transduction. To this end, we have characterized the molecular processes associated with rAAV transduction and integration within sets of normal and AT primary fibroblasts and transformed cell lines. Our data demonstrate a significant enhancement of rAAV transduction and integration in ATM deficient cell lines, accompanied by an altered profile for UV-induced rAAV transduction. We propose a hypothesis whereby the mutated ATM gene affects the abundance or activity of DNA repair enzymes involved in the formation of rAAV circular intermediates and concatamers, which enhance the levels of integration and transgene expression. These results further our understanding of mechanisms involved in rAAV transduction and genome conversion.

RESULTS

rAAV transduction is enhanced in ATM-deficient fibroblasts

Genotoxic agents have been reported to augment rAAV transduction through an unknown mechanism. Because AT patients are defective in DNA repair, we tested whether rAAV vectors have an altered transduction profile in ATM-deficient cell lines compared with their wild-

type counterparts. To test this hypothesis, we used an rAAV vector, AV.GFP3ori, that harbors the GFP reporter transgene. To our surprise, an AT transformed cell line, GM5849, demonstrated a 5- to 7-fold increased susceptibility for rAAV transduction in comparison with the wild-type control cell line, GM637, at m.o.i. values ranging from 10 to 100 DNA particles/cell (Fig. 1A). These results suggested that AT cells possess enhanced pathways for rAAV transduction.

AT cell lines have an altered rAAV transduction profile in response to UV irradiation

AT cells are known to display sensitivity to ionizing radiation (Taylor *et al.*, 1975). In addition, genotoxic agents such as UV irradiation have been reported to augment rAAV transduction (Miller *et al.*, 1997; Sanlioglu *et al.*, 1999). Because AT cells displayed augmented rAAV transduction, we hypothesized that the mechanism normally underlying the UV enhancement of rAAV transduction may preexist in these cells. To investigate this hypothesis, both wild-type and AT-transformed fibroblasts were UV irradiated at increasing doses before infection with AV.GFP3ori at an m.o.i. of 100 DNA particles/cell (Fig. 1B). A 4- to 5-fold induction in GFP expression was obtained with wild-type fibroblasts at 15 and 25 J/m² UV over nonirradiated controls. In contrast, no significant enhancement in rAAV transduction was observed in AT GM5849 cells by UV irradiation over all the doses tested (Fig. 1B).

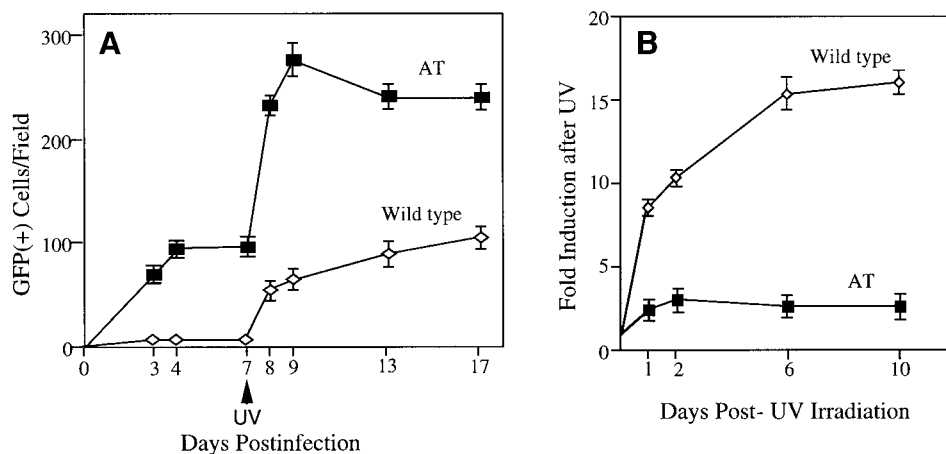


FIG. 2. rAAV transduction in primary fibroblasts isolated from AT patients. Three independent isolates of primary AT (GM01740A, GM01829A, GM00648C) and wild-type (GM00023, GM00041B, GM00495A) human fibroblasts were evaluated for the efficiency of rAAV transduction (A). Infections were carried out in triplicate with increasing doses of rAAV virus (only m.o.i. of 200 DNA particles/cell is shown). The mean \pm SEM ($n = 9$) number of GFP-positive cells/20 \times field (y-axis) is given at various times postinfection (x-axis) for the three fibroblast lines evaluated each group. At 7 days postinfection, cells were UV irradiated at 25 J/m² (indicated by an arrow). The fold induction in rAAV transduction after UV irradiation is given in panel B (fold increase was calculated using expression at 7-day time point equal to 1). Similar results for UV induction were seen when cells were UV irradiated before infection (data not shown).

Primary fibroblast cells isolated from AT patients demonstrate similar alterations in rAAV transduction

To confirm that the observed phenotype of enhanced rAAV transduction and reduced UV response was not restricted to the selected transformed cell lines used in these experiments, rAAV transduction was evaluated in primary fibroblasts isolated from AT and normal patients. Three primary AT cells (GM01740A, GM01829A, GM00648C) and three primary wild-type cells (GM00023, GM00041B, GM00495A) were used. As seen in Fig. 1C, the enhanced, baseline susceptibility of AT primary fibroblasts to rAAV infection was even greater than that in transformed AT cell lines. AT primary cells infected with AV.GFP3ori virus (m.o.i. of 200 DNA particles/cell) demonstrated a 16-fold higher level of transduction than their wild-type fibroblast controls. Furthermore, UV irradiation before rAAV infection lead to a 17-fold enhancement in GFP expressing cells only in wild-type fibroblasts (Fig. 1C). In contrast, AT fibroblasts demonstrated a minimal 2-fold enhancement in transduction after UV irradiation. These results demonstrate common patterns of rAAV transduction in primary AT fibroblasts and transformed cell lines, suggesting that the ATM deficiency affects both the baseline and UV-facilitated rAAV transduction events.

Transcriptionally inactive rAAV genomes are stably maintained in normal fibroblasts, and their conversion to transcriptionally active forms is enhanced by UV irradiation and the ATM deficiency

We hypothesized that ATM gene defects accounting for enhanced baseline levels of rAAV transduction and

gene expression might lead to altered activity of DNA repair enzymes capable of increasing the rate of single-stranded rAAV genome conversion to double-stranded expressible forms. This hypothesis suggests that infection and uptake of virus are equivalent in AT and normal cells and that events occurring subsequent to viral infection are responsible for the observed alterations in the transduction profiles. To test whether rAAV genomes persist in normal cells in a transcriptionally inactive state after infection, the effect of UV irradiation administered 7 days after infection on rAAV transduction was evaluated in both AT and normal cell lines. Both AT and normal fibroblasts were infected and incubated for 24 h with AV.GFP3 ori, followed by washing. The medium was then changed and the cells were incubated for an additional 6 days. On day 7 after infection, AT cells demonstrated a 16-fold greater transduction than normal fibroblasts, as evidenced by the number of GFP-expressing cells (Fig. 2A). However, in normal fibroblasts, UV irradiation at this time point was capable of inducing GFP expression from transcriptionally inactive rAAV genomes more than 17-fold, whereas AT fibroblasts exhibited only a 2-fold increase in response to UV (Figs. 2A and 2B). From these results, we concluded that in wild-type fibroblasts, rAAV genomes remained in an inactive state that could be rescued by UV irradiation. In contrast, processes responsible for UV augmentation of transcriptionally inactive rAAV genomes appear to pre-exist in nonirradiated AT cells. This is indicated by the findings that AT cells show a high baseline level of transduction and a blunted response to UV irradiation administered at 7 days postinfection.

Mechanism of rAAV transduction in ATM-deficient cell lines

Binding and uptake of viral DNA are equivalent in normal and AT fibroblasts. Although UV rescue experiments indicated that rAAV genomes remained in a transcriptionally inactive state within infected wild-type fibroblasts, we wanted to rule out that differences in baseline transduction levels in AT compared with wild-type fibroblasts were due to differential uptake and accumulation of AAV ssDNA. To address this question, we analyzed the molecular state of the viral DNA using Southern blots of Hirt DNA purified 1, 5, and 24 h subsequent to infection. The results demonstrated no detectable difference in the accumulation of viral DNA between AT and wild-type cells (data only shown for 24-h time points in Fig. 3A). This suggests that binding and uptake of virus are equivalent for both AT and normal fibroblasts.

Conversion of single-stranded rAAV genomes to circular forms is elevated in ATM cells. Although the abundance of single-stranded rAAV genomes was equivalent in AT and normal cells, the Southern blots demonstrated several distinct differences between these two cell types (Fig. 3A). First, as previously reported (Sanlioglu *et al.*, 1999), the abundance of supercoiled circular AAV genomes (migrating at 2.8 kb) was significantly induced in normal fibroblasts by UV irradiation at 25 J/m². In contrast, AT cell lines demonstrated elevated levels of circular form genomes compared with wild-type cells in the absence of UV irradiation. In addition, UV irradiation increased the abundance of a higher-molecular-weight (6 kb) genome fragment of rAAV in AT cells (Fig. 3A). Both monomer circular form genomes (2.8 kb) and this higher-molecular-weight 6-kb band demonstrated migration patterns distinct from rAAV replication form monomers (Rfm, 4.7 kb) and dimers (Rfd, 9.4 kb) (Ferrari *et al.*, 1996; Fisher *et al.*, 1996).

UV enhances the formation of rAAV circular concatamers in AT cells. We hypothesized that the larger 6-kb band induced by UV irradiation of rAAV-infected AT cells represents an alternative form of circular genome (i.e., dimer or relaxed monomer). To test this hypothesis, Hirt DNA was size fractionated, and an enriched fraction containing the 6-kb genomic fragment was isolated for restriction enzyme analysis (Fig. 3B). *Asel* digestion of the purified 6-kb Hirt DNA band from AT cells yielded a 4.7-kb fragment consistent with a uniform circular head-to-tail dimer. Furthermore, *Pst*I digestion generated two fragments of 3 and 1.7 kb. Last, three fragments of 1.7, 1.5, and 1.36 kb were obtained by *Asel*-*Pst*I double digestion. In conclusion, these restriction digestion patterns support the identity of the 6-kb fragment as a circular form dimer. End fragments that would be consistent with a linear head-to-tail concatamer were not seen. Similarly, digestion patterns consistent with replication form intermediates were also not observed. A schematic representation of restriction fragments that would arise from

circular forms and/or replication forms of AAV is depicted in Fig. 3C.

These observations were also confirmed by rescue assays of circular form genomes after transformation of *Escherichia coli* Sure cells with Hirt DNA. Because only closed circular form rAAV genomes are capable of giving rise to CFU after bacterial transformation (Duan *et al.*, 1998), we digested Hirt DNA with *Asel* before transformation to determine the abundance of closed circular form genomes in Hirt DNA. Results from these studies demonstrate $1.2 \times 10^4 \pm 400$ (mean \pm SEM) rescued bacterial colonies from mock digested AT Hirt DNA (total colonies per 60-mm plate) in the absence of *Asel* enzyme. In contrast, *Asel* digestion of Hirt DNA before transformation completely eliminated all rescued plasmids from our assay. In summary, results of Hirt DNA Southern blots and plasmid rescue assays provide good evidence that the conversion products of rAAV genomes (2.8- and 6-kb bands) in AT cells are indeed uniform head-to-tail circular genomes.

rAAV integration is elevated in ATM-deficient cells

Our results thus far demonstrate that the conversion process of ssDNA rAAV genomes to circular concatamers is elevated in ATM-deficient cells. We hypothesized that circular form genomes and/or the concatamerization process of these circular forms may be associated with mechanisms of integration. Several lines of evidence support the notion that large circular concatamers may be preintegration intermediates for rAAV. For example, the proviral structure of rAAV in liver (Miao *et al.*, 1998) and other cell lines (Duan *et al.*, 1997; Laughlin, Cardellio, and Coon, 1986; Tratschin *et al.*, 1985) consists of uniform head-to-tail concatamers. To test the hypothesis that increased abundance of circular form genomes in AT cells predisposes rAAV to a higher level of integration, we compared the extent of GFP-expressing clone formation in AV.GFP3ori-infected AT cells (GM5849) with that in wild-type cells (GM637). GFP colonies were quantified at various passages postinfection, and clones were isolated for analysis by Southern blotting at passage 7. As shown in Figs. 4A and 4B, the number of clones was stable between passages 4 and 7, suggesting that integration had taken place. Interestingly, the number of clones seen in the AT GM5849 cell line was 7-fold higher than that in normal GM637 cells. This increase correlated with a higher abundance of circular form genomes in these cell lines after rAAV infection. Because UV irradiation induces circular form AAV genomes in non-AT cells, we compared clone formation in UV-irradiated rAAV-infected AT and normal cells to determine any differences in the extent of clone formation. Results from this analysis demonstrated a 4-fold increase in the number of GFP-expressing colonies in normal GM637 cells after UV irradiation. In contrast, no significant increase in colony formation was seen in UV-irradiated rAAV-in-

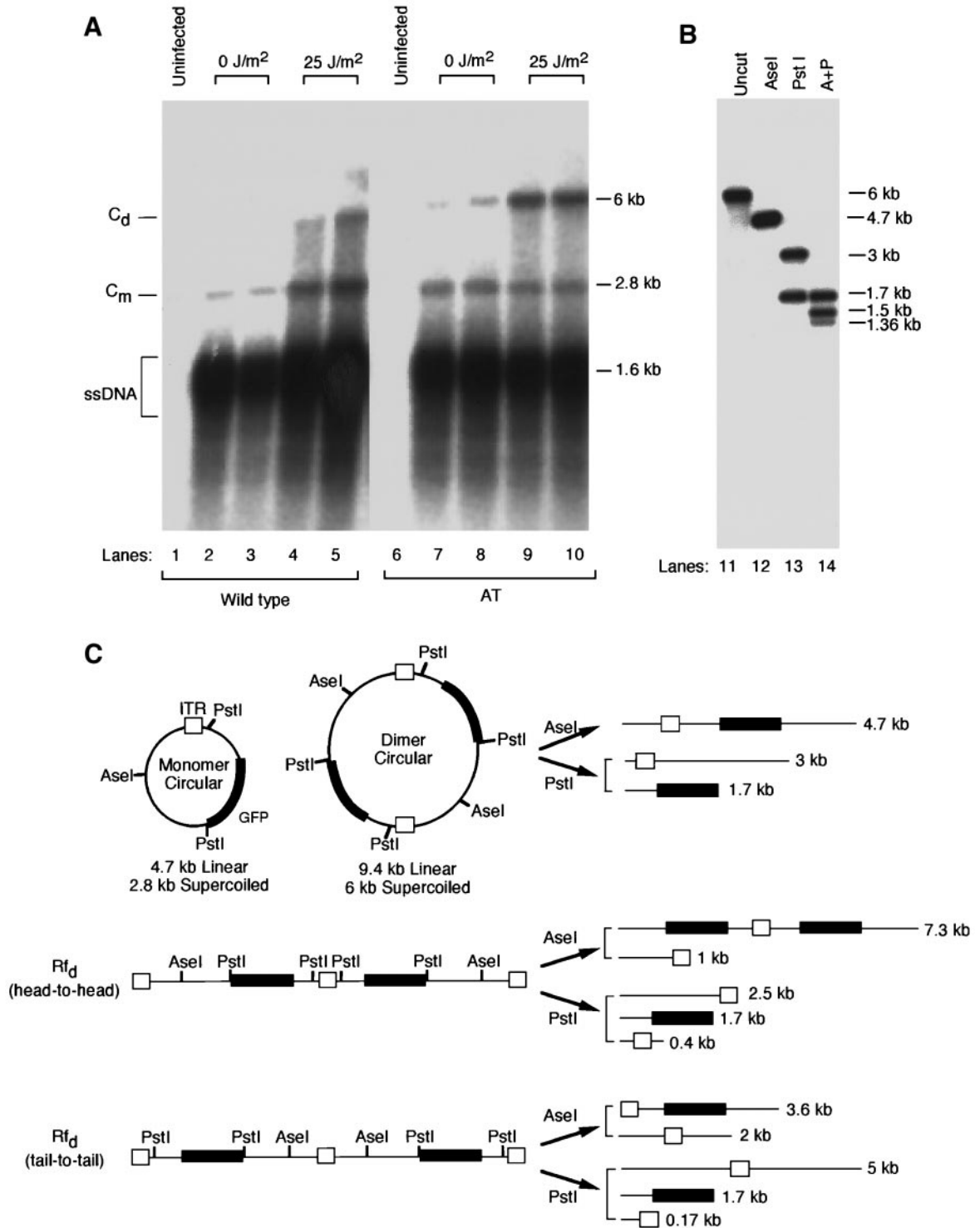


FIG. 3. Enhanced rAAV transduction in AT cells is reflected by an increased abundance of circular form rAAV genomes. AT (GM5849) and wild-type (GM637) transformed fibroblasts were infected with AV.GFP3ori virus at an m.o.i. of 100 DNA particles/cell. The abundance of rAAV circular intermediates was determined by Hirt Southern blot analysis at 24 h postinfection as described in Materials and Methods (A). Southern blotting analysis was performed with a ³²P-labeled GFP fragment (820 bp *EcoRI* and *NotI* fragment) of pEGFP-1 (Clontech). Lanes 1–10 represent undigested Hirt DNA from uninfected controls (lanes 1 and 6) and rAAV-infected cells (lanes 2–5 and 7–10) preirradiated with 0 and 25 J/m² (paired lanes represent duplicate independent samples). The corresponding molecular weight for various forms of the AAV genome is given on the right in kb. Nomenclature to the left of panel A depicts C_d (circular dimers), C_m (circular monomers), and ssDNA (of rAAV). (B) Restriction enzyme analysis of fractionated 5- to 7-kb Hirt DNA shown in panel A (25 J/m² infected AT cells). The Southern blot in Panel B used ³²P-labeled intact circular viral genome as probe. Purified uncut Hirt DNA ran as a single 6-kb fragment (lane 11). *AseI* digestion (lane 12) yielded only a 4.7-kb fragment. *PstI* digestion (lane 13) yielded 3- and 1.7-kb fragments. *AseI*-*PstI* double digestion generated 1.7-, 1.5-, and 1.36-kb fragments (lane 14). (C) Schematic representation of expected digestion patterns with single enzymes shown in panel B. Monomer and dimer supercoiled circular forms of the rAAV genome migrate as 2.8 and 6 kb,

fectured AT GM5849 cells. Despite the UV-induced increase in stable clone formation seen in wild-type cells, the number of GFP-positive clones in irradiated wild-type cells remained 40% lower than that of nonirradiated AT cells. These results suggest that the ATM deficiency augments mechanisms that facilitate rAAV integration.

Structural analysis of integrated rAAV genomes

To confirm that GFP clones (Fig. 4B) possessed integrated copies of the rAAV genome, clones were isolated and expanded for preparation of genomic DNA. Southern blot analysis of undigested DNA samples demonstrated large-molecular-weight bands usually retained in the loading well, consistent with integrated genomes or high-molecular-weight concatamers (Fig. 4C, U). However, *HindIII* digestion (*HindIII* does not cut within the rAAV genome) of genomic DNA demonstrated unique single sites of integration within each of the four clones analyzed (Fig. 4C, lanes 2–5). Detailed structural analysis of one such clone presented in Fig. 4C (lanes 7–10) confirmed the head-to-tail orientation of rAAV genomes. This was expected if they had arisen from circular concatamers. In this clone, *HindIII* digestion yielded a single fragment (>16 kb) suggestive of a single integration site. *Asel* digestion (which cuts once in the viral genome) released a fragment of 4.7 kb, suggestive of head-to-tail concatamers, and a 12-kb fragment of flanking sequence with less intense hybridization. Copy number standards (Fig. 4C, p80) suggested that this proviral integration site contained approximately three or four copies of the AAV genome. The orientation of these integrated rAAV genomes was confirmed by *Asel*–*PstI* double digestion (Fig. 4C, lane 10). The presence of 1.7-, 1.5-, and 1.36-kb fragments confirms the head-to-tail orientation of these genomes. For comparison of head-to-tail digestion patterns seen in a circular genome, a rescued circular intermediate (p80) is also shown in Fig. 4C (lanes 11–13). These results confirm that clones evaluated in our system have integrated copies of rAAV and that the structure is of these proviruses is consistent with head-to-tail circular intermediates as preintegration molecular forms of the rAAV genome.

Trafficking of rAAV to the nucleus is unaffected by the AT phenotype

Several mechanisms that could explain the increased abundance of rAAV circular intermediates in AT cells might involve increased binding, endocytosis, and/or nuclear trafficking of virus. Our Southern blot

data (Fig. 3A) demonstrating equivalent accumulation of rAAV ssDNA in wild-type and AT cells after infection suggests that binding and endocytosis are likely not different in these two cell types. However, it remains a formal possibility that altered efficiencies of nuclear trafficking of virus could explain increased transduction in AT cells. For example, in wild-type cells, rAAV might be trapped in an endosomal compartment that is liberated after UV irradiation. To address this question, we evaluated the intracellular trafficking of Cy3-labeled rAAV in both AT and wild-type cells. Cy3AAV was incubated with AT cells (GM5849) and wild-type cells (GM637) at 4°C for 1 h. Cells were then immediately fixed to examine viral binding or incubated at 37°C for 2 h to analyze nuclear trafficking. As shown in Fig. 5, no difference in binding of Cy3AAV was detected between wild-type (Figs. 5A and 5B) and AT cells (Figs. 5C and 5D). In addition, we have previously determined that the majority of rAAV particles are transported to the nucleus within a 2-h time frame (data not shown). Therefore, we compared the efficiency of nuclear transport of Cy3AAV in AT and wild-type cells 2 h after the infection. As seen in Fig. 5, Cy3AAV was efficiently transported to the nucleus in both wild-type (Figs. 5E and 5F) and AT cells (Figs. 5G and 5H). Therefore, we conclude that the observed difference in transduction between AT and wild-type cells cannot be due to differences in the efficiency of binding, endocytosis, or nuclear transport but instead must involve nuclear mechanisms.

Tyrosine dephosphorylation of a single-stranded D box binding protein (ssD-BP) has been correlated with the efficiency of rAAV transduction in certain cell types and tissues (Qing *et al.*, 1998, 1997; Sanlioglu and Engelhardt, 1999). Thus we examined the phosphorylation status of ssD-BP in AT and wild-type cells by performing mobility shift assays (Sanlioglu and Engelhardt, 1999). However, no significant difference in the ratio of dephosphorylated (–P) to phosphorylated (+P) forms of ssD-BP in these two cell types was found (data not shown). Hence, we conclude that the phosphorylation status of ssD-BP does not account for the differences in transduction. In conclusion, the only observable difference between AT and wild-type cells is the relative abundance of AAV circular intermediates. The exact mechanism responsible for higher abundance of AAV circular intermediates observed in AT cells, however, remain to be determined.

respectively. Both circular forms yield a 4.7-kb linearized rAAV genome fragment after digestion with *Asel* enzyme. These fragment sizes can be differentiated from the expected molecular weight digestion fragments of Rf_h head-to-head (7.3 and 1 kb) and tail-to-tail (3.6 and 2 kb) genomes. *PstI* digestion of the circular form dimer generates 3- and 1.7-kb fragments, whereas an Rf head-to-head dimer would yield 2.5-, 1.7-, and 0.4-kb fragments and Rf tail-to-tail dimer would generate 5-, 1.7-, and 0.17-kb fragments. Schematic representation of the *Asel*–*PstI* double digestion was omitted for the purpose of clarity.

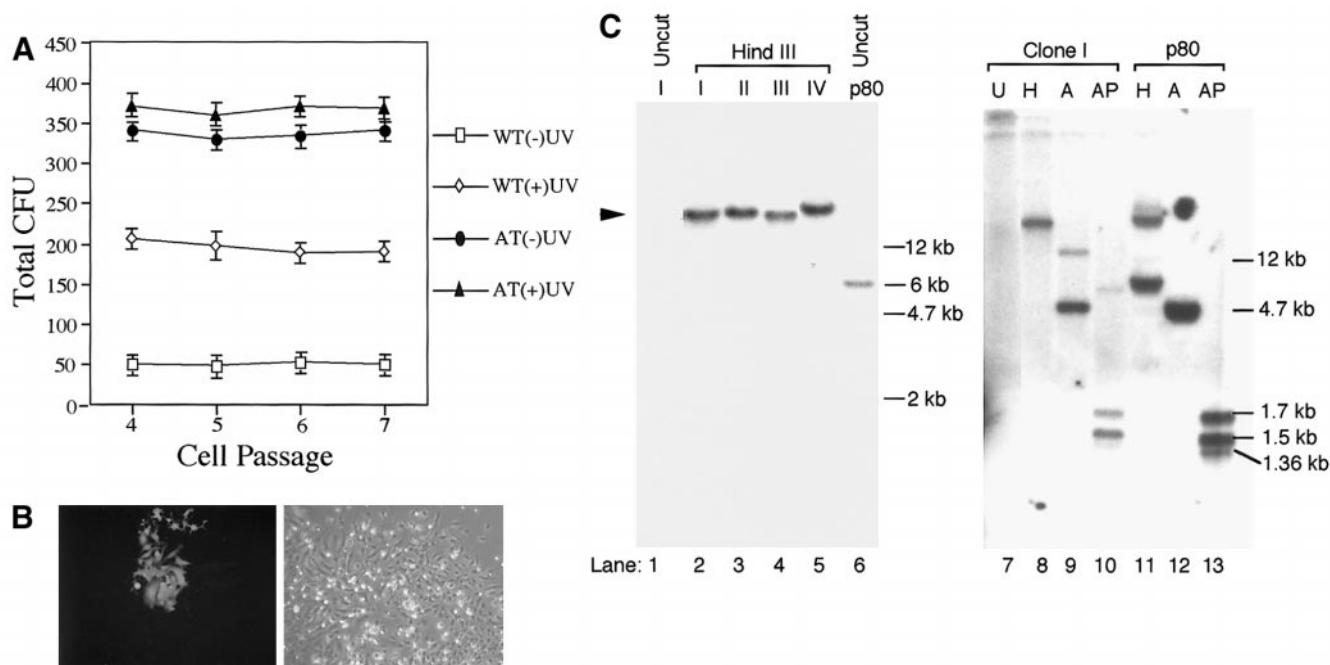


FIG. 4. rAAV integration in AT cells and wild-type fibroblasts. Wild-type (GM637) and AT (GM5849) transformed fibroblasts were infected with rAAV virus at an m.o.i. of 500 DNA particles/cell with and without prior UV irradiation at 25 J/m². After several cell passages (1/20 split each passage, GFP-positive colonies; CFU) were counted on triplicate 100-mm plates only when cells became confluent (A). These results represent the mean \pm SEM of three different experiments ($n = 9$). A representative photomicrograph of a GFP-positive clone is given in panel B. To confirm that these clones had integrated copies of rAAV, clones were isolated and expanded for preparation of genomic DNA and Southern blot analysis (C). Southern blotting of uncut (lane 1) and *Hind*III-digested (lanes 2–5) genomic DNA is shown for four independently isolated clones I–IV (*Hind*III does not cut within the viral genome). As a control for episomal dimer circular rAAV genomes (6 kb), the rescued circular intermediate plasmid p80 was also *Hind*III digested and run in lane 6. The arrowhead marks linear *Hind*III genomic fragments of rAAV genomes at a molecular weight greater than 16 kb. A more detailed restriction map of genomic DNA from clone I is given in lanes 7–10 and compared with that of p80 (lanes 11–13). U, undigested; H, *Hind*III (no site in rAAV); A, *Ase*I (a single site in AAV); AP, *Ase*I–*Pst*I double digest. All Southern blots were probed with a ³²P-labeled *Ase*I fragment of the circular intermediate plasmid p80. Molecular weights are given in kb to the right gels in panel C. A detailed restriction map of AV.GFP3ori virus is described elsewhere (Duan *et al.*, 1998).

DISCUSSION

In addition to adenovirus E4 gene expression, genotoxic agents such as ionizing radiation, UV, and hydroxyurea have also been shown to increase rAAV transduction (Alexander *et al.*, 1994; Ferrari *et al.*, 1996; Fisher *et al.*, 1996; Russell *et al.*, 1995). However, the mechanisms accounting for this enhanced transduction are not clearly understood. Because DNA damage is a common feature of these genotoxic agents, DNA repair pathways activated by DNA damage are thought to be involved in this augmentation process (Alexander *et al.*, 1994). Therefore, we hypothesized that the investigation of genetically mutant cell lines with modulated DNA repair pathways may lend insight into genotoxic mechanisms that enhance rAAV transduction. ATM deficiency is one such example of a mutant DNA repair phenotype that leads to enhanced sensitivity to ionizing radiation through a defective cell cycle checkpoint pathway (Taylor *et al.*, 1975).

Initial studies in transformed cell lines confirmed this hypothesis and demonstrated a 5-fold increase in baseline rAAV transduction in AT compared with wild-type transformed fibroblasts. Further investigation in three

primary fibroblast lines from both AT and normal individuals substantiated these findings and demonstrated a 16-fold higher baseline transduction of rAAV associated with the AT phenotype. Interestingly, genotoxic stress caused by UV irradiation was capable of increasing rAAV transduction in wild-type cells without significant enhancement in AT primary fibroblasts. These studies confirmed that ATM deficiency plays a role in altering the cellular milieu in a manner conducive to rAAV transduction.

Several lines of evidence suggest that the ATM deficiency alters the transduction processes of rAAV through an enhanced conversion of viral ssDNA to circular form genomes. These processes, which are enhanced in AT cells, appear to be similar to those induced by UV in non-AT cell lines (Fig. 6). Based on Southern blot analysis of Hirt DNA, no difference in the extent of accumulated single-stranded rAAV genomes was observed between wild-type and AT cell lines after a 24-h infection, suggesting that equivalent molar amounts of viral DNA are taken up by these two genetically different cells lines. Interestingly, these transcriptionally inactive single-stranded rAAV genomes appear to be quite stable in

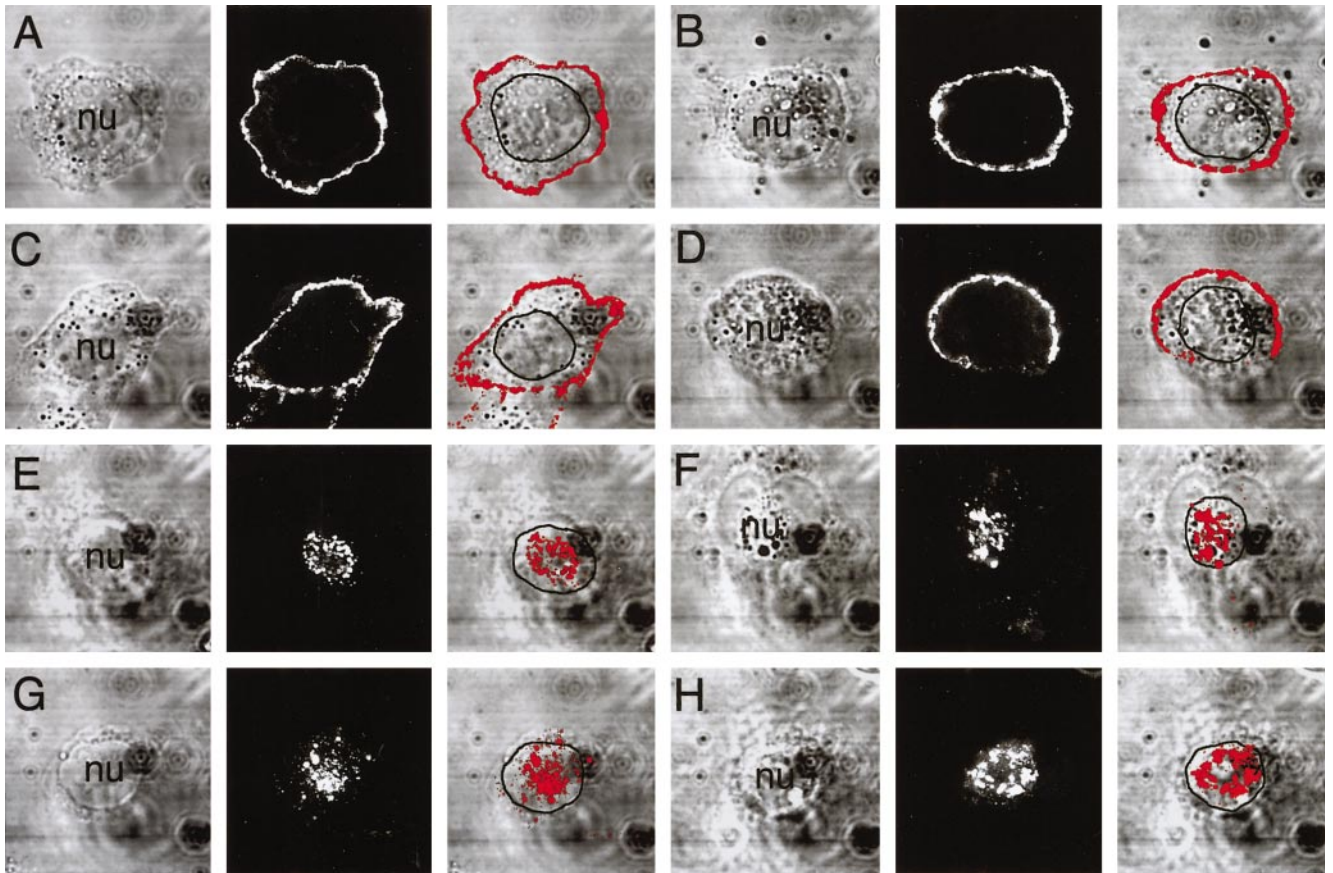


FIG. 5. Endocytic trafficking of Cy3AAV. Cy3AAV was incubated with fibroblasts grown on glass slides at 4°C for 1 h to allow virus to bind. Cells were then either fixed immediately (A–D) or incubated for an additional 2 h at 37°C (E–H). Confocal photomicrographs of Cy3AAV-infected wild-type fibroblast cell line GM637 (A, B, E, and F) and AT fibroblast cell line GM5849 (C, D, G, and H) are shown. Each of the panels gives a confocal phase contrast image to visualize cellular boundaries (left), gray scale image of rhodamine channel (middle), and superimposed images (right). Two representative confocal photomicrographs are given for each time point. Each image is a stack of three 0.5- μm consecutive layers. The boundary of the nucleus (nu) in the superimposed image is also marked for clarity.

cells after the infection of wild-type cells, as evidenced by successful gene conversion to circular intermediates after UV irradiation 7 days after infection. Based on the findings that the efficiency of binding, endocytosis, and nuclear transport of Cy3AAV are equivalent in both wild-type and AT cells, we conclude that enhanced transduction in AT cells occurs through a nuclear-mediated mechanism. This would be consistent with the hypothesis that UV irradiation activates enzymes responsible for the conversion of viral ssDNA to circular genomes and that the AT defect elevates these same enzymes. However, the phosphorylation status of ssD-BP, which is not significantly different in AT and wild-type cells, suggests that some other protein must be involved.

In summary, these data suggest that AT cells express the cellular machinery necessary to convert single-stranded rAAV DNA into circular form genomes more efficiently than wild-type fibroblasts. Moreover, as shown by clonal expansion studies, this increase in circular rAAV genomes correlates with enhanced integration of rAAV in ATM-deficient cell lines. However, a similar enhancement in the abundance of rAAV circular intermedi-

ates, with concordant increases in integration, was achieved by UV irradiation of wild-type cells before rAAV infection. The fact that UV irradiation did not induce similar changes in AT cells suggests that pathways for gene conversion and integration of rAAV may already be maximal in AT cells. Southern blot analysis of genomic DNA structurally supports the hypothesis that circular form genomes are preintegration intermediates (Fig. 5). These studies suggest new insights into rAAV transduction pathways that control second-strand synthesis and integration. Furthermore, the fact that the ATM gene deficiency enhances this process provides new avenues for discovering cellular factors to augment gene transfer with rAAV vectors.

MATERIALS AND METHODS

Generation of recombinant AAV stocks

The *cis*-acting plasmid (pCisAV.GFP3ori) that was used for rAAV production has been described previously (Duan *et al.*, 1998). Recombinant AAV2 stocks were generated by cotransfection of pCisAV.GFP3ori and pRep/

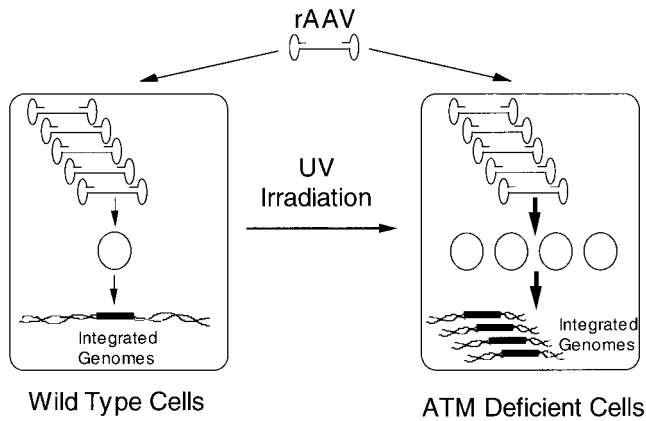


FIG. 6. A model for AT genotype-dependent enhancement of rAAV transduction. After infection of both AT and wild-type fibroblasts, equivalent amounts of ssDNA can be detected in Hirt DNA. These data suggest that the uptake of virus is not altered by the AT phenotype. However, in the absence of UV irradiation, the abundance of rAAV circular form genomes is significantly higher in AT cells compared with wild type. This enhanced conversion of ssDNA viral genomes correlates with an increased level of transgene expression in AT cells in the absence of UV. In contrast, UV irradiation enhanced both the abundance of monomer circular rAAV genomes and transgene expression in wild-type but not AT cells. Furthermore, the efficiency of circular rAAV genome formation appears to be linked to a concatamerization process that facilitates integration. This is indicated by the finding that in the absence of UV, AT cells have a 7-fold higher extent of rAAV integration than wild-type cells. UV irradiation of wild-type cells appears to augment cellular processes similar to the pathways responsible for increased circular intermediate formation and integration in ATM-deficient cells.

Cap together with coinfection with recombinant Ad.CMVlacZ in 293 cells (Fisher *et al.*, 1996). The AV.GFP3ori virus was subsequently purified through three rounds of CsCl banding, followed by heat inactivation of contaminating adenovirus at 60°C for 1 h. DNA titers were determined by viral DNA slot blot hybridization against a EGFP P³²-labeled probe with copy number plasmid standards. Typical yields from viral preparations were 2×10^{12} DNA particles/ml. The absence of helper adenovirus was confirmed by histochemical staining of rAAV-infected 293 cells for β -galactosidase, and no recombinant adenovirus was found in 10^{10} particles of purified rAAV stocks (limits of sensitivity of assay). Similarly, assays for wild-type AAV performed as previously described (Duan *et al.*, 1998) confirmed less than 1 wild-type functional particle in 10^{10} particles of purified rAAV stocks (limits of sensitivity of assay).

Cy3 Labeling of rAAV

Purified rAV.GFP3ori was conjugated with the bifunctional NHS-ester carbocyanine-Cy3 using a modification of a procedure from Amersham (Arlington Heights, IL). This protocol conjugates Cy3 to amine groups in viral capsid proteins through ester linkages. Purified rAAV was dialyzed and concentrated in conjugation buffer using Centricon 30 ultrafilters (Millipore Corporation,

Bedford, MA) before the labeling reaction. The lyophilized Cy3 dye was also dissolved in conjugation buffer (0.1 M sodium carbonate, pH 9.3). Briefly, samples of virus (5×10^{11} particles) were incubated for 30 min at room temperature with NHS-ester carbocyanine-Cy3 dye in a reaction volume of 1 ml. The solutions were then transferred to dialysis chambers (10,000 molecular weight cutoff; GIBCO BRL, Grand Island, NY) and dialyzed for 24 h against two changes of buffer containing 20 mM HEPES, pH 7.5, and 150 mM NaCl. Last, the samples were dialyzed in DMEM with no serum overnight and concentrated in a Centricon 30. GFP titers of Cy3-labeled virus were approximately 80% that of mock-labeled virus. This Cy3 virus solution was used directly to infect the wild-type fibroblast cell line GM637 or the AT fibroblast cell line GM5849 grown on glass slides at 4°C for 60 min (in the absence of serum). After 4°C binding of the labeled virus, slides were washed in serum-free medium two times and either fixed in 2% paraformaldehyde for analysis or shifted to 37°C for continued infection in the presence of medium containing 10% serum. Dye-to-protein ratios (D/P) were calculated according to the manufacturer's instructions (Amersham Life Science, Clearbrook, IL) and were approximately equal to 1.

Cell lines, infection procedures, and transduction assays

All of the cell lines used in this study, including the transformed AT fibroblast cell line GM5849, primary AT cell fibroblasts (GM01740A, GM01829A, GM00648C), transformed wild-type fibroblast cell line GM637, and wild-type primary fibroblasts (GM00023, GM00041B, GM00495A), were obtained from Coriel Cell Repositories (Camden, NJ). AT (GM5849) and wild-type (GM637) transformed fibroblasts were plated onto 60-mm plates at 48 h before infection. When cells reached confluency (2×10^6 cells/60-mm plate), they were infected with rAAV virus (AV.GFP3ori) in DMEM with 2% FBS for 2 h. After 2 h of exposure to the virus, the serum concentration was increased to a final concentration of 10% by adding DMEM with 20% FBS. The efficiency of rAAV transduction was determined at 24, 48, and 72 h after infection. Because transduction reached a plateau by 24 h postinfection, the percentage of GFP-positive cells was determined by FACS analysis at this time. For UV irradiation experiments, cells were UV irradiated at increasing doses (0, 5, 15, and 25 J/m²) using a Stratagene Stratalinker (La Jolla, CA) and were then infected with AV.GFP3ori virus at an m.o.i. of 100 DNA particles/cell. The percentage of cells expressing GFP was determined 24 h after the infection by FACS analysis. For AT primary cell fibroblasts (GM01740A, GM01829A, GM00648C) and wild-type primary fibroblasts (GM00023, GM00041B, GM00495A), experiments were performed on 6-well plates at 72 h post-confluency. Cells were UV irradiated (25 J/m²) either

before infection with AV.GFP3ori virus or at 7 days postinfection. The transduction efficiency was quantified by counting the number of positive cells per 20× field at various time points before and after UV irradiation.

Hirt Southern blotting analysis

Hirt DNA was isolated according to modifications of previously described protocols at 24 h after infection with rAAV (Duan *et al.*, 1998; Hirt, 1967). In brief, cells were trypsinized, pelleted, and stored at -80°C before the Hirt procedure. Cells were then resuspended in 320 μl of Hirt extraction buffer containing 10 mM Tris and 10 mM EDTA, pH 8.0. Then 1 μl of DNase-free RNase (10 mg/ml) and 36 μl of 10% SDS were added to samples, and cells were incubated at 37°C for 0.5 h. Samples were further treated with 1 mg/ml Pronase and 20 $\mu\text{g/ml}$ proteinase K for 2 h at 37°C . After the addition of NaCl to a final concentration of 1.1 M, samples were incubated at 4°C overnight. Samples were then centrifuged for 30 min at 4°C , and the supernatant was removed, extracted with phenol-chloroform, and precipitated in 100% EtOH in the presence of 1 μl of 10 mg/ml yeast tRNA overnight at -20°C . After centrifugation for 30 min, pellets were washed with 70% ethanol, and the pellet was dried and resuspended in 50 μl of water. Then 10 μl of each sample was electrophoresed on 0.8% agarose gels, and Southern blots were hybridized to ^{32}P -labeled EGFP probes.

Fractionation of AAV circular concatamer genomes from Hirt DNA

The AT fibroblast cell line GM5849 was infected with rAAV virus at an m.o.i. of 25,000 DNA particles/cell after UV irradiation at 25 J/m^2 . Hirt DNA was then isolated at 24 h postinfection. Hirt DNA was fractionated in a 0.8% agarose gel, and DNA ranging from 5 to 7 kb (based on 1-kb DNA ladder) was excised and electroeluted into low-salt buffer containing 20 mM Tris-Cl, pH 7.0, 5 mM NaCl, and 0.2 mM EDTA. Samples were extracted in phenol-chloroform, concentrated by butanol extraction, and finally ethanol precipitated in the presence of excess yeast tRNA. Then 1 μg of mouse genomic DNA was added before restriction enzyme digestion to prevent nonspecific degradation of small amounts of Hirt DNA. Southern blotting was performed using a ^{32}P -labeled intact AAV circular viral genome rescued from *E. coli* (p80).

Colony forming assays

Because assays for integration require continuous cell passaging and the growth of primary AT fibroblasts is limited to several passages, transformed AT and normal cell lines were used in our integration assays. No difference was observed in growth rates between the transformed cell lines (wild-type GM637 and AT GM5849 cells). Cells (1×10^6 ; wild-type-GM637 or AT-GM5849)

were plated onto 60-mm plates. On the next day, confluent monolayers were UV irradiated at 25 J/m^2 , followed by infection with AV.GFP3ori virus at an m.o.i. of 100 and 500 DNA particles/cell. Since the same correlation was observed between the two m.o.i. values tested, we only report the results of infections performed at m.o.i. values of 500 DNA particles/cell. Control infections in the absence of UV irradiation were also performed. At 24 h post infection, cells were trypsinized and plated onto 100-mm plates. At confluency, cells were serially passaged by diluting cells 1:20 each time. Equal numbers of cells were passaged each time. After the fourth passage, clones were clearly visible. Clones were quantified after each subsequent passage by fluorescent microscopy only when cells were confluent. After the seventh passage, GFP positive colonies were harvested and expanded for Southern blot analysis of genomic DNA.

Genomic DNA preparation and Southern blotting

Genomic DNA preparations were prepared from expanded GFP-positive clones in a confluent 100-mm dish. Briefly, cells were incubated in digestion buffer containing 100 mM NaCl, 10 mM Tris-Cl, pH 8, 25 mM EDTA, pH 8, 0.5% SDS, and 0.1 mg/ml proteinase K overnight at 50°C . After phenol-chloroform extractions (twice), genomic DNA was precipitated by adding one-half volume of 7.5 M ammonium acetate and 2 volumes of ethanol. After washing samples with 70% ethanol, DNA was dissolved in ddH₂O by incubation at 65°C for 30 min. Then 10 μg of genomic DNA for each sample was digested with *Hind*III, *Ase*I, or *Ase*I-*Pst*I restriction enzymes and resolved on a 1% agarose gel. As a control for head-to-tail proviral structure, the p80 plasmid, a rescued circular, head-to-tail AAV genome, was also digested and run on Southern blots. Southern blots were probed with a ^{32}P -labeled DNA fragment of the intact viral genome originating from linearized (*Ase*I digested) p80.

ACKNOWLEDGMENTS

We thank Dr. Terry Ritchie for her useful discussions and editorial comments. The work described here was supported by National Institutes of Health Grant R01-DK/HL58340 (J.F.E.) and the Gene Therapy Core Center cofunded by the National Institute of Diabetes and Digestive and Kidney Diseases and the Cystic Fibrosis Foundation (Grant DK54759)

REFERENCES

- Alexander, I. E., Russell, D. W., and Miller, A. D. (1994). DNA-damaging agents greatly increase the transduction of nondividing cells by adeno-associated virus vectors. *J. Virol.* **68**, 8282–8287.
- Banin, S., Moyal, L., Shieh, S., Taya, Y., Anderson, C. W., Chessa, L., Smorodinsky, N. I., Prives, C., Reiss, Y., Shiloh, Y., and Ziv, Y. (1998). Enhanced phosphorylation of p53 by ATM in response to DNA damage. *Science* **281**, 1674–1677.
- Barlow, C., Brown, K. D., Deng, C. X., Tagle, D. A., and Wynshaw-Boris, A. (1997). ATM selectively regulates distinct p53-dependent cell-cycle checkpoint and apoptotic pathways [published erratum appears in *Nat. Genet.* (1998). 18:298]. *Nat. Genet.* **17**, 453–456.

- Berns, K. I. (1990). Parvovirus replication. *Microbiol. Rev.* **54**, 316–329.
- Canman, C. E., Lim, D. S., Cimprich, K. A., Taya, Y., Tamai, K., Sakaguchi, K., Appella, E., Kastan, M. B., and Siliciano, J. D. (1998). Activation of the ATM kinase by ionizing radiation and phosphorylation of p53. *Science* **281**, 1677–1679.
- Duan, D., Fisher, K. J., Burda, J. F., and Engelhardt, J. F. (1997). Structural and functional heterogeneity of integrated recombinant AAV genomes. *Virus Res.* **48**, 41–56.
- Duan, D., Sharma, P., Yang, J., Yue, Y., Dudus, L., Zhang, Y., Fisher, K. J., and Engelhardt, J. F. (1998). Circular intermediates of recombinant adeno-associated virus have defined structural characteristics responsible for long term episomal persistence in muscle. *J. Virol.* **72**, 8568–8577.
- Ferrari, F. K., Samulski, T., Shenk, T., and Samulski, R. J. (1996). Second-stranded synthesis is a rate-limiting step for efficient transduction by recombinant adeno-associated virus vectors. *J. Virol.* **70**, 3227–3234.
- Fisher, K. J., Gao, G. P., Weitzman, M. D., DeMatteo, R., Burda, J. F., and Wilson, J. M. (1996). Transduction with recombinant adeno-associated virus for gene therapy is limited by leading-stranded synthesis. *J. Virol.* **70**, 520–532.
- Flotte, T. R., Afione, S. A., and Zeitlin, P. L. (1994). Adeno-associated virus vector gene expression occurs in nondividing cells in the absence of vector DNA integration. *Am. J. Respir. Cell Mol. Biol.* **11**, 517–521.
- Hirt, B. (1967). Selective extraction of polyoma DNA from infected mouse cell cultures. *J. Mol. Biol.* **26**, 365–369.
- Jung, M., Kondratyev, A., Lee, S. A., Dimtchev, A., and Dritschilo, A. (1997). ATM gene product phosphorylates I kappa B-alpha. *Cancer Res.* **57**, 24–27.
- Kapeller, R., and Cantley, L. C. (1994). Phosphatidylinositol 3-kinase. *Bioessays* **16**, 565–576.
- Kaplitt, M. G., Leone, P., Samulski, R. J., Xiao, X., Pfaff, D. W., O'Malley, K. L., and Doring, M. J. (1994). Long-term gene expression and phenotypic correction using adeno-associated virus vectors in the mammalian brain. *Nat. Genet.* **8**, 148–154.
- Kastan, M. B., Zhan, Q., el-Deiry, W. S., Carrier, F., Jacks, T., Walsh, W. V., Plunkett, B. S., Vogelstein, B., and Fornace, A. J., Jr. (1992). A mammalian cell cycle checkpoint pathway utilizing p53 and GADD45 is defective in ataxia-telangiectasia. *Cell* **71**, 587–597.
- Kotin, R. M., Menninger, J. C., Ward, D. C., and Berns, K. I. (1991). Mapping and direct visualization of a region-specific viral DNA integration site on chromosome 19q13-qter. *Genomics* **10**, 831–834.
- Laughlin, C. A., Cardellicchio, C. B., and Coon, H. C. (1986). Latent infection of KB cells with adeno-associated virus type 2. *J. Virol.* **60**, 515–524.
- Lu, H., Taya, Y., Ikeda, M., and Levine, A. J. (1998). Ultraviolet radiation, but not gamma radiation or etoposide-induced DNA damage, results in the phosphorylation of the murine p53 protein at serine-389. *Proc. Natl. Acad. Sci. USA* **95**, 6399–6402.
- Luo, C. M., Tang, W., Mekeel, K. L., DeFrank, J. S., Anne, P. R., and Powell, S. N. (1996). High frequency and error-prone DNA recombination in ataxia telangiectasia cell lines. *J. Biol. Chem.* **271**, 4497–4503.
- McCown, T. J., Xiao, X., Li, J., Breese, G. R., and Samulski, R. J. (1996). Differential and persistent expression patterns of CNS gene transfer by an adeno-associated virus (AAV) vector. *Brain Res.* **713**, 99–107.
- Miao, C. H., Snyder, R. O., Schowalter, D. B., Patijn, G. A., Donahue, B., Winther, B., and Kay, M. A. (1998). The kinetics of rAAV integration in the liver [letter]. *Nat. Genet.* **19**, 13–15.
- Miller, S. C., Taylor, A., Watanabe, K., Mok, K., and Torti, F. M. (1997). Regulation of NF-kappaB and HIV-1 LTR activity in mouse L cells by ultraviolet radiation: LTR trans-activation in a nonirradiated genome in heterokaryons. *Exp. Cell Res.* **230**, 9–21.
- Nakamura, Y. (1998). ATM: The p53 booster [news]. *Nat. Med.* **4**, 1231–1232.
- Qing, K., Khuntirat, B., Mah, C., Kube, D. M., Wang, X. S., Ponnazhagan, S., Zhou, S., Dwarki, V. J., Yoder, M. C., and Srivastava, A. (1998). Adeno-associated virus type 2-mediated gene transfer: Correlation of tyrosine phosphorylation of the cellular single-stranded D sequence-binding protein with transgene expression in human cells in vitro and murine tissues in vivo. *J. Virol.* **72**, 1593–1599.
- Qing, K., Wang, X. S., Kube, D. M., Ponnazhagan, S., Bajpai, A., and Srivastava, A. (1997). Role of tyrosine phosphorylation of a cellular protein in adeno-associated virus 2-mediated transgene expression. *Proc. Natl. Acad. Sci. USA* **94**, 10879–108784.
- Russell, D. W., Alexander, I. E., and Miller, A. D. (1995). DNA synthesis and topoisomerase inhibitors increase transduction by adeno-associated virus vectors. *Proc. Natl. Acad. Sci. USA* **92**, 5719–5723.
- Sanlioglu, S., Duan, D., and Engelhardt, J. F. (1999). Two independent molecular pathways for recombinant adeno-associated virus genome conversion occur after UV-C and E4orf6 augmentation of transduction. *Hum. Gene Ther.* **10**, 591–602.
- Sanlioglu, S., and Engelhardt, J. (1999). Cellular redox state alters recombinant adeno-associated virus transduction through tyrosine phosphatase pathways. *Gene Ther.* **6**, 1427–1437.
- Savitsky, K., Bar-Shira, A., Gilad, S., Rotman, G., Ziv, Y., Vanagaite, L., Tagle, D. A., Smith, S., Uziel, T., Sfez, S., and et al. (1995). A single ataxia telangiectasia gene with a product similar to PI-3 kinase [see comments]. *Science* **268**, 1749–1753.
- Shiloh, Y. (1995). Ataxia-telangiectasia: Closer to unraveling the mystery. *Eur. J. Hum. Genet.* **3**, 116–138.
- Shiloh, Y. (1997). Ataxia-telangiectasia and the Nijmegen breakage syndrome: Related disorders but genes apart. *Annu. Rev. Genet.* **31**, 635–662.
- Taylor, A. M., Harnden, D. G., Arlett, C. F., Harcourt, S. A., Lehmann, A. R., Stevens, S., and Bridges, B. A. (1975). Ataxia telangiectasia: A human mutation with abnormal radiation sensitivity. *Nature* **258**, 427–429.
- Tratschin, J. D., Miller, I. L., Smith, M. G., and Carter, B. J. (1985). Adeno-associated virus vector for high-frequency integration, expression, and rescue of genes in mammalian cells. *Mol. Cell. Biol.* **5**, 3251–3260.
- Ui, M., Okada, T., Hazeki, K., and Hazeki, O. (1995). Wortmannin as a unique probe for an intracellular signalling protein, phosphoinositide 3-kinase. *Trends Biochem. Sci.* **20**, 303–307.
- Walsh, C. E., Liu, J. M., Xiao, X., Young, N. S., Nienhuis, A. W., and Samulski, R. J. (1992). Regulated high level expression of a human gamma-globin gene introduced into erythroid cells by an adeno-associated virus vector. *Proc. Natl. Acad. Sci. USA* **89**, 7257–7261.
- Whitman, M., Downes, C. P., Keeler, M., Keller, T., and Cantley, L. (1988). Type I phosphatidylinositol kinase makes a novel inositol phospholipid, phosphatidylinositol-3-phosphate. *Nature* **332**, 644–646.